LYMPHOID NEOPLASIA

C1013G/CXCR4 acts as a driver mutation of tumor progression and modulator of drug resistance in lymphoplasmacytic lymphoma

Aldo M. Roccaro,[1] Antonio Sacco,[1] Cristina Jimenez,[2] Patricia Maiso,[1] Michele Moschetta,[1] Yuji Mishima,[1] Yosra Aljawai,[1] Ilyas Sahin,[1] Michelle Kuhne,[3] Pina Cardarelli,[3] Lewis Cohen,[4] Jesus F. San Miguel,[5] Ramon Garcia-Sanz,[2] and Irene M. Ghobrial[1]

[1]Department of Medical Oncology, Dana-Farber Cancer Institute, Harvard Medical School, Boston, MA; [2]University of Salamanca, Salamanca, Spain; [3]Bristol-Myers Squibb, Redwood City, CA; [4]Bristol-Myers Squibb, Lawrenceville, NJ; and [5]University of Navarra, Pamplona, Spain

Key Points

- C1013G/CXCR4 acts as an activating mutation in WM leading to enhanced tumor growth, and as an inducer of drug resistance.
- BMS936564/MDX1338, a novel anti-CXCR4 moAb, successfully targets WM cells, either C1013G/CXCR4 mutated or wild-type.

The C-X-C chemokine receptor type 4 (CXCR4) plays a crucial role in modulating cell trafficking in hematopoietic stem cells and clonal B cells. We screened 418 patients with B-cell lymphoproliferative disorders and described the presence of the C1013G/CXCR4 warts, hypogammaglobulinemia, infections, and myelokathexis–associated mutation in 28.2% (37/131) of patients with lymphoplasmacytic lymphoma (Waldenström macroglobulinemia [WM]), being either absent or present in only 7% of other B-cell lymphomas. In vivo functional characterization demonstrates its activating role in WM cells, as demonstrated by significant tumor proliferation and dissemination to extramedullary organs, leading to disease progression and decreased survival. The use of a monoclonal antibody anti-CXCR4 led to significant tumor reduction in a C1013G/CXCR4 WM model, whereas drug resistance was observed in mutated WM cells exposed to Bruton's tyrosine kinase, mammalian target of rapamycin, and phosphatidylinositol 3-kinase inhibitors, but not proteasome inhibitors. These findings demonstrate that C1013G/CXCR4 is an activating mutation in WM and support its role as a critical regulator of WM molecular pathogenesis and as an important therapeutic target. (*Blood*. 2014;123(26):4120-4131)

Introduction

Whole-genome sequencing has recently enhanced our understanding of the molecular mechanisms that may contribute to the pathogenesis of Waldenström macroglobulinemia (WM). Specifically, L265P/MYD88 has been described as a prevalent somatic mutation in WM patients.[1] In vitro studies have demonstrated that the L265P/MYD88 variant may lead to increased tumor cell proliferation [2]; this may be explained, at least in part, by MYD88-dependent activation of nuclear factor κB (NF-κB), a known signaling pathway that modulates tumor B-cell survival, growth, and resistance to therapy.[3] These observations are also consistent with previous findings that overexpression of the oncogenic microRNA-155 in clonal WM cells leads to activation of NF-κB in primary WM cells. Indeed, microRNA-155 loss-of-function studies led to inhibition of NF-κB and reduction of tumor growth in vitro and in vivo.[3,4] However, MYD88 mutation did not predict progression or resistance to therapy in several published studies, indicating that other genetic alterations may be critical for tumor progression and dissemination to distant organs. Among low-grade B-cell lymphomas, WM represents a lymphoplasmacytic subtype characterized by bone marrow (BM) infiltration of lymphoplasmacytic cells and secretion of a serum monoclonal immunoglobulin M (IgM) protein.[5,6] The evidence for widespread involvement of the BM at the time of diagnosis implies cell trafficking of clonal B cells into the BM. In this context, 1 of the main regulators of tumor B-cell homing to the BM is represented by CXCR4 through the interaction with its related ligand stromal derived factor-1 (SDF-1/CXCL12). CXCR4 plays also a crucial role in physiological conditions, such as lymphopoiesis and BM myelopoiesis, during embryogenesis. During the postnatal life, CXCR4 and its ligand modulate homing of $CD34^+$ cells to the BM niches as well as lymphocytic trafficking. CXCR4 has been shown to be mutated in patients with an inherited heterozygous autosomal dominant disease characterized by aberrantly functioning immunity, known as warts, hypogammaglobulinemia, infections, and myelokathexis (WHIM) syndrome, because of the presence, among others, of an activating mutation of the CXCR4 gene, represented by the C1013G variant.[7,8] Recent evidences support the presence of CXCR4 somatic aberrations in WM.[9,10] The functional role of this variant in supporting progression of lymphoplasmacytic lymphoma and whether it is peculiar for WM or it occurs at an IgM monoclonal gammopathy of undetermined significance (MGUS) stage compared with other

Submitted March 24, 2014; accepted April 3, 2014. Prepublished online as *Blood* First Edition paper, April 7, 2014; DOI 10.1182/blood-2014-03-564583.

A.M.R. and A.S. contributed equally to this study.

The online version of this article contains a data supplement.

There is an Inside *Blood* Commentary on this article in this issue.

The publication costs of this article were defrayed in part by page charge payment. Therefore, and solely to indicate this fact, this article is hereby marked "advertisement" in accordance with 18 USC section 1734.

B-cell lymphoproliferative entities has not been previously described. We therefore investigated the presence of the C1013/CXCR4 variant in 418 patients with different B-cell lymphoproliferative disorders and aimed to define the in vivo functional role of this variant in WM. The present studies confirmed that 28.2% of WM patients (37/131) harbor this specific variant; demonstrating its activating role as shown in vivo in a C1013G/CXCR4 WM model. Based on these findings, we tested a monoclonal antibody anti-CXCR4 (BMS936564/MDX1338) and found its antitumor activity directed against both C1013G/CXCR4-mutated and wild-type WM cells. Importantly, C1013G/CXCR4-mutated cells presented with resistance to conventionally used anti-WM small molecules, such as mammalian target of rapamycin (mTOR), Bruton's tyrosine kinase (BTK), and phosphatidylinositol 3-kinase (PI3K) inhibitors.

Methods

Clinical samples

Tumor samples were collected at the Department of Hematology, Salamanca, Spain, from 4118 patients with different B-cell lymphoproliferative disorders, distributed as follows: Waldenström macroglobulinemia (n = 137), IgM MGUS (n = 40), diffuse large B-cell lymphoma (n = 75), splenic marginal zone lymphoma (n = 14), B-cell chronic lymphocytic lymphoma (n = 37, including 16 with M-component), hairy cell leukemia (n = 35), multiple myeloma (n = 36, 3 of IgM isotype), IgA/IgG MGUS (n = 22), lymphoplasmacytic lymphoma with no WM criteria (n = 13), amyloidosis (n = 6), and B-cell lymphoproliferative disorders not otherwise specified (n = 9). Diagnosis was made according to the latest World Health Organization classification of tumors of hematopoietic and lymphoid tissues.[11] Thirty-two healthy volunteers were also included in the study as controls. Immunophenotypic evaluation was done using conventional methods, panels of monoclonal antibodies previously described,[12] and following the general recommendations of the EuroFlow group for the immunophenotypic evaluation of hematological malignancies.[13] These cases were immunophenotyped using 4-color combinations that included up to 20 different antigens in addition to surface IgM) and cytoplasmatic Ig λ and κ. The percentage of clonal cells was counted with the tube including the surface IgM/CD25/CD19/CD38 MoAb. Data acquisition was performed in a FACSCalibur flow cytometer (Becton Dickinson Biosciences, San Jose, CA) using the FACSDiva software (version 6.1; Becton Dickinson Biosciences), and a 2-step acquisition procedure for total and CD19$^+$-only events. Data analysis was performed using Infinicyt software (Cytognos; Salamanca, Spain). After immunophenotypic analysis, clonal cell quantification in diagnostic tissues and detection of the C1013G/CXCR4 variant was performed using real-time allele-specific polymerase chain reaction (PCR). Ten cases of extramedullary WM were also included in these studies. Approval was obtained from the Dana-Farber Cancer Institute and the University Hospital of Salamanca Institutional Review Boards for these studies. Informed consent was provided according to the Declaration of Helsinki.

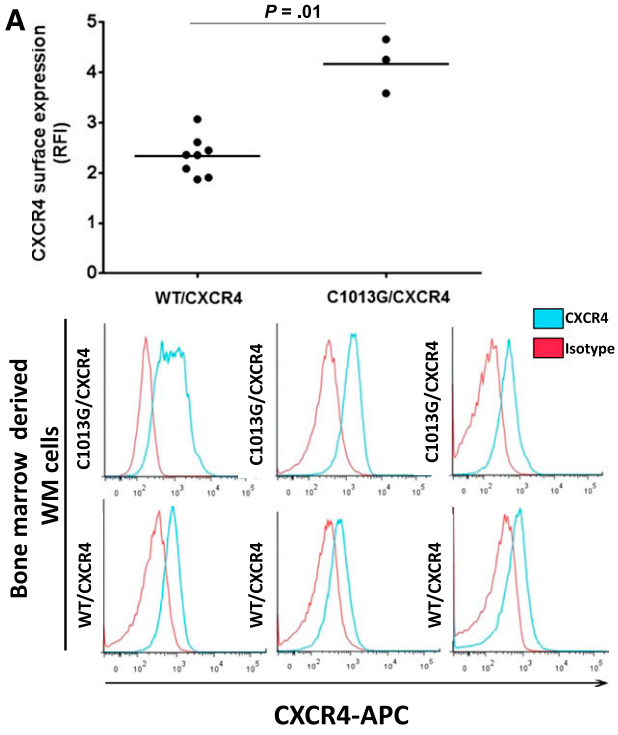

B

	C1013G/CXCR4	Wild type/CXCR4
Lung (n=3)	3/3	0
Kidney (n=1)	1/1	0
Small bowel (n=2)	0	2/2
Soft tissues (n=4)	0	4/4

Figure 1. Identification of the somatic C1013G/CXCR4 variant in WM patients. (A) Primary WM samples harboring the C1013G/CXCR4 variant present with higher CXCR4 surface expression compared with wild-type (WT) primary WM samples, as shown by flow cytometry on CD19$^+$ BM-derived WM cells. (B) The C1013G/CXCR4 variant is present in lung and kidney tissues of patients with extramedullary WM disease. The variant has been detected by ASO-PCR using genomic DNA. RFI, relative fluorescence intensity.

Table 1. WM patients present with C1013G/CXCR4 somatic mutation

		CXCR4 C1013G	
Entity	N = 418	No.	Percent
WM	131	37	28.2
IgM MGUS	40	8	20
Diffuse large cell lymphoma	75	1	1.3
Splenic marginal zone lymphoma	14	1	7
B-CLL (16 with monoclonal component)	37	0	0
Hairy cell leukemia	35	0	0
Multiple myeloma (3 with IgM)	36	0	0
IgA/IgG MGUS	22	0	0
Lymphoplasmacytic lymphoma (with no WM criteria)	13	0	0
Amyloidosis	6	0	0
B-CLL disorder, NOS	9	0	0
Healthy volunteers	32	0	0

C1013G/CXCR4 variant occurs in 28% of patients with WM, being either absent or present in a minority of patient with B-cell lymphoproliferative disorders.

B-CLL, B-cell chronic lymphocytic leukemia; MGUS, monoclonal gammopathy of undetermined significance; NOS, not otherwise specified.

Real-time ASO-PCR for CXCR4 C1013G identification in diagnostic tissues

A real-time allele-specific oligonucleotide PCR (ASO-PCR) was developed based on the use of 2 reverse primers differing in the 2 last nucleotides (at the 3′ position) so that they are specific either of the wild-type or the mutated allele, as described.[12] To prevent the amplification of the nonmatching primer (increasing specificity), an additional nucleotide mismatch (C>G) was introduced next to the mutated base. The specific length and position of the

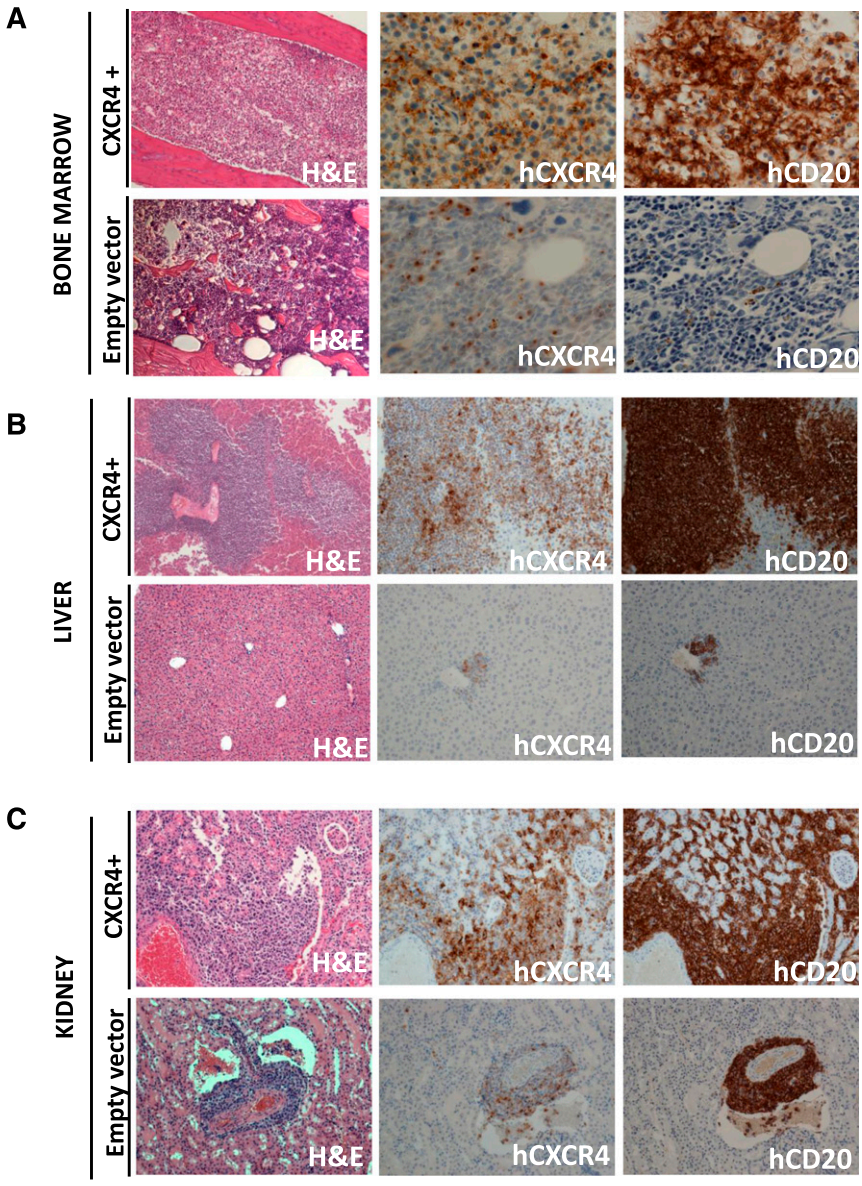

Figure 2. Overexpression of CXCR4 in WM cells leads to increased disease dissemination in vivo and enhanced adhesion properties and growth in vitro. CXCR4 overexpressing cells ($CXCR4^+$) presented with a more aggressive ability to disseminate to BM (A), liver (B), and kidneys (C) compared with the related empty vector–infected cells (Hematoxylin Eosin ×10; Ab staining ×20 and ×10, magnifications). Quantification of human CD20 and CXCR4 staining is shown in supplemental Figure 2. In addition, $CXCR4^+$ and control cells were detected ex vivo by using immunofluorescence on BM, liver, and kidney tissues (D) (×10 and ×20 magnifications). (E) Kaplan-Meier curve showing decreased survival in $CXCR4^+$ cell–injected mice vs empty vector cell–injected mice (n = 7/group). Death for empty vector cell–injected mice was observed at days 40, 50, and 62. *P* indicates *P* value (log-rank test). (F-G) CXCR4 overexpression led to increased WM cell adhesion to primary BM-MSCs, and increased cell proliferation in contrast with CXCR4-silenced WM cells (CXCR4-K.D.), in which reduced adhesion to BM-MSCs and reduced cell proliferation were observed. Bars indicate standard deviation. DAPI, 4′,6 diamidino-2-phenylindole; NS, not significant.

primers were calculated with Oligo 6.0 software (Molecular Biology Insights, Cascade, CO). Reverse primers were: 5′-GACTCAGACTCAGTGGAAA CAGATG-3′ (reverse wild-type primer) and 5′-GACTCAGACTCAGTG GAAACAGAAC-3′ (reverse mutated primer). The common forward primer was 5′-TTTCTTCCACTGTTGTCTGAACC-3′, for a final 165-bp PCR product. In addition, a specific TaqMan probe was designed for such a PCR with the Primer Express Software, v3.0.1 (Applied Biosystems, Foster City, CA), which yielded the following reporter, sequence and quencher: 6FAM:5′-TATGCTTTCCTTGGAGCCA-3′:NFQ-MGB.

For real-time ASO-PCR development, each experiment required 2 different PCR reactions: 1 for the detection of the CXCR4 C1013G mutation (with the mutated reverse primer) and the other as a control of the DNA quality (using the wild-type reverse primer). Each reaction was carried out in a final volume of 20 μL, containing 300 nM of each primer, 200 nM of the probe, 1× of the TaqMan Universal PCR Master Mix (Applied Biosystems), and 20 ng of genomic DNA.

Experiments were performed in a StepOnePlus Real-Time PCR System (Applied Biosystems) and consisted of an initial denaturation step of 10 minutes at 95°C, followed by 50 cycles of 95°C for 15 seconds and 60°C for 60 seconds. Data were analyzed with StepOne Software, v2.1 (Applied Biosystems).

Immunohistochemistry and immunofluorescence

Murine tissues (BM, liver, kidney, lung, lymph nodes) were analyzed and quantified for the expression of human CD20 and human CXCR4. Immunofluorescence imaging was performed for the evaluation of green fluorescence protein $(GFP)^+$/CXCR4 overexpressing WM cells or red fluorescence protein $(RFP)^+$/empty-vector WM cells.

C1013G/CXCR4 mutagenesis

C1013G/CXCR4 variant was generated in WM cell lines (BCWM.1; MWCL1) by site-directed mutagenesis using the QuickChange XL site-directed mutagenesis kit (Stratagene; Agilent Technologies, Santa Clara, CA), according to the manufacturer's instructions. Cells infected with a control vector were considered as control and are presented within this article as "control cells."

In vivo studies

SCID/Bg mice (n = 5 per group) were injected with BCWM.1 infected with either precision LentiORF/CXCR4/GFP ($CXCR4^+$)- or empty vector/RFP (control)-infected BCWM.1 cells. After 3 weeks, mice were euthanized and

Figure 2. (Continued).

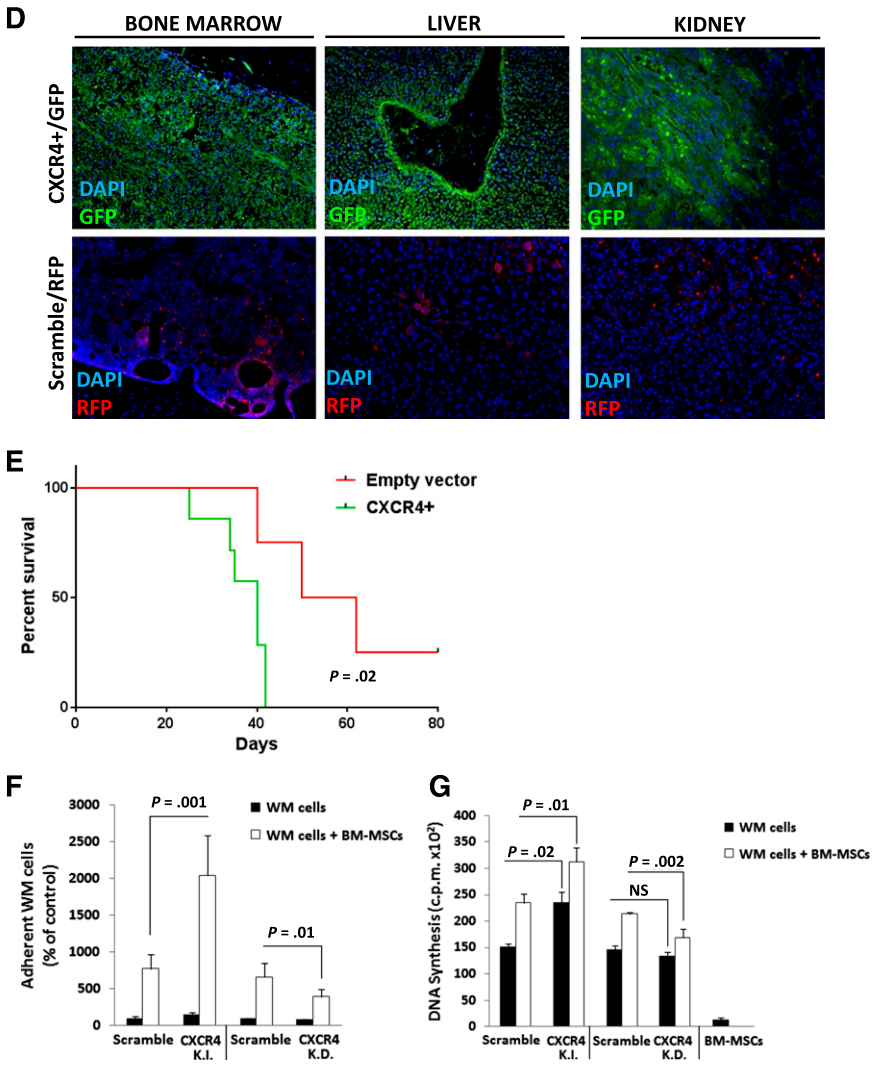

organs harvested. Hematoxylin-eosin staining and immunohistochemistry for human CD20 and CXCR4 were performed on explanted organs. Independent experiments were conducted to evaluate differences in survival (SCID/Bg mice, n = 7/group). Similar studies were conducted using C1013/CXCR4-mutated cells and control vector–infected cells (control cells). Independent experiments were conducted to evaluate differences in survival (SCID/Bg mice, n = 7/group). In vivo homing studies were performed using BCWM.1-mCherry^{+} cells: cells were injected IV into SID/Bg mice and treated with either BMS936564MDX1338 or control antibody (10 mg/kg, intraperitoneally; 3-4 times per week for 3 weeks). The ability of BMS936564/MDX1338 to modulate WM homing to BM, spleen, and lymph nodes was evaluated ex vivo at the third week on explanted tissues by using fluorescence microscope (Eclipse 80i; Nikon, Melville, NY).[14]

Activity of BMS936564/MDX1338 was tested in SCID/Bg mice injected with C1013G/CXCR4-mutated cells. Mice controls were treated with an isotype control antibody (n = 5 mice/group; BMS936564MDX1338) or control antibody (10 mg/kg, intraperitoneally; 3-4 times per week for 3 weeks).

Gene expression studies

Gene expression profile was performed on C1013G/CXCR4-mutated BCWM.1 cells, using HG-U133 plus 2 Array (GSE50683). RNA was isolated using RNeasy kit (Qiagen). Data were normalized using *d*-Chip software. Differentially expressed gene signatures were analyzed using Gene Set Enrichment Analysis (GSEA) and considered significant with a false discovery rate (FDR) <0.25, as previously reported.[15] Gene sets were downloaded from a publically available source (Broad Institute, Cambridge, MA).

In vitro cell adhesion, migration, survival, and proliferation studies

CXCR4 gain or loss of function studies were performed using WM cell lines (BCWM.1; MWCL1), either alone or in the context of primary WM BM mesenchymal stromal cells (BM-MSCs), as previously described.[16,17] CXCR4 was knocked down in WM cells using short hairpin RNAs (clones 171, 649) and lentivirus-mediated infection; scramble probe was used as control (Thermo Scientific, Waltham, MA) containing the target sequence (clones 171, 649) or scramble control, according to manufacturer's specifications. Transduction efficiency was performed by using quantitative reverse-transcription PCR (qRT-PCR) and by evaluating the detection of GFP-expressing cells by using a fluorescence microscope (Nikon Eclipse 80i). Overexpression of CXCR4 was obtained in WM cells using either precision LentiORF/CXCR4/GFP (CXCR4^{+}) or empty vector/RFP used as control (Thermo Scientific). Overexpression efficiency was performed by using qRT-PCR and by detecting GFP- and RFP-expressing cells by using a fluorescence microscope (Nikon Eclipse 80i; Nikon, Melville, NY). Adhesion assay was performed on WM cells using fibronectin-coated plates, according to the manufacturer's recommendations (EMD Biosciences, San Diego, CA) and as described.[16,17] Adhesion of WM cells to primary WM BM-MSCs cells was tested as previously described.[16-18] WM cell proliferation was assessed

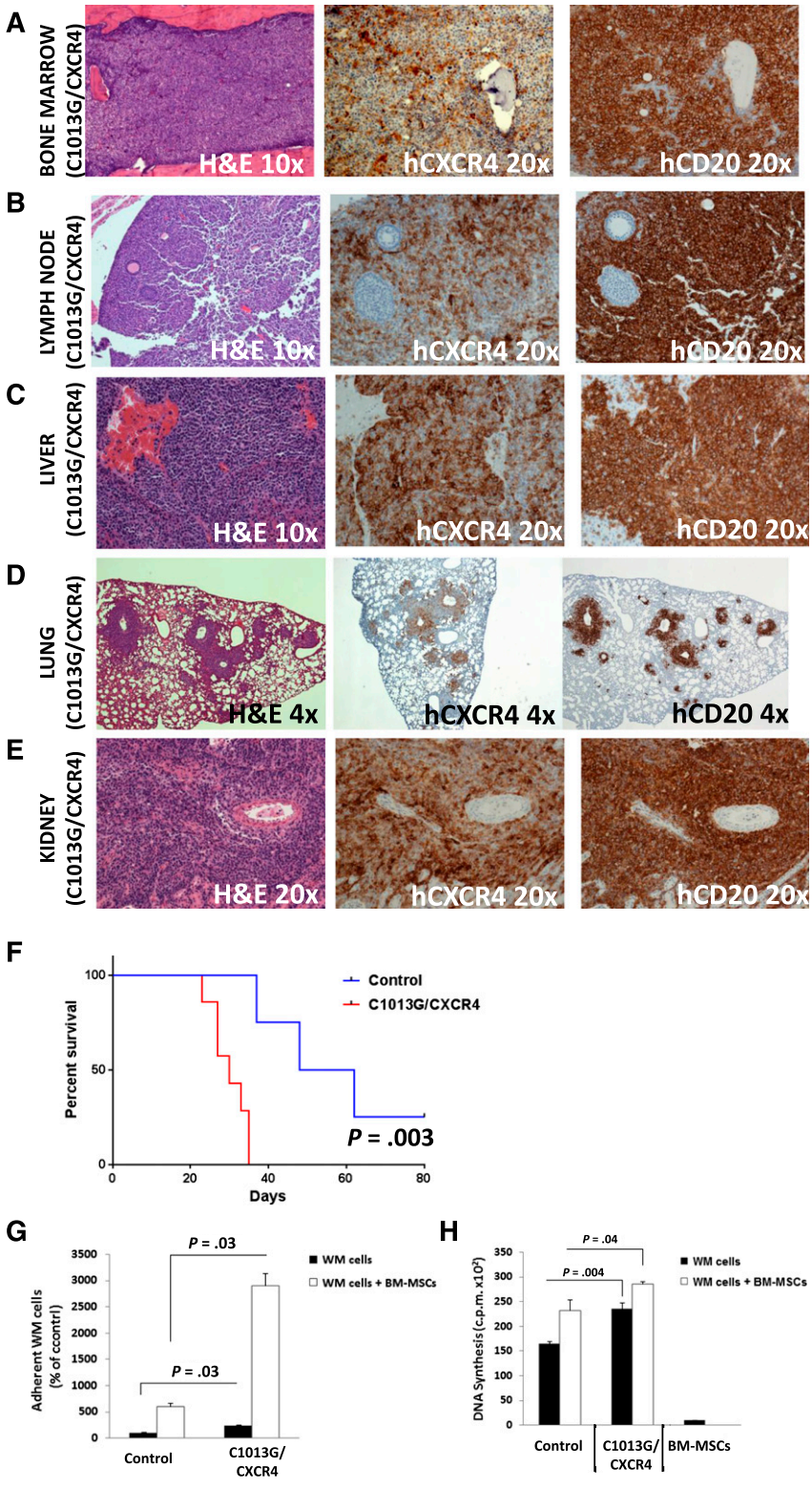

Figure 3. CXCR4/C1013G mutation drives dissemination of WM cells in vivo. WM cells harboring the C1013G/CXCR4 variant present with changes at the mRNA level, together with increased cell adhesion and cell proliferation. SCID/Bg mice injected IV with C1013G/CXCR4 variant-harboring WM cells presented with significant involvement of (A) BM, (B) lymph nodes, (C) liver, (D) lung, (E) kidneys (×4, ×10, and ×20 magnifications). Quantification of human CD20 and CXCR4 staining is shown in supplemental Figure 4. (F) Kaplan-Meier curve showing decreased survival in C1013G/CXCR4 cell–injected mice vs control vector cell–injected mice (n = 7/group). Death for control vector cell–injected mice was observed at days 37, 48, and 62. (G-H) C1013G/CXCR4 variant increased adhesion and proliferation of WM cells either alone or in the context of BM-MSCs. Bars indicate standard deviation. *P* indicates *P* values.

evaluating DNA synthesis, measured by [^{3}H]-thymidine uptake, after 48 hours of coculture with primary BM-MSCs, as previously described.[16-18] Cell toxicity was evaluated by measuring 3-(4,5-dimethylthiazol-2-yl)-2,5-diphenyltetrazolium bromide (Chemicon International, Temecula, CA), as described.[16-18] Migration assay was performed using transwell migration plates (Corning Life Sciences, Tewksbury, MA), as previously reported.[16-18]

Reagents

Everolimus, idelalisib, ibrutinib, bortezomib, and carfilzomib were purchased from Selleck Chemicals (Houston, TX). Drugs were dissolved in dimethylsulfoxide and subsequently diluted in cell culture medium (10% fetal bovine serum) immediately before use. The maximum final concentration of dimethylsulfoxide (<0.1%) did not affect cell proliferation and did not induce

cytotoxicity on the cell lines tested. BMS936564/MDX-1338 and the control human IgG4 isotype control were obtained from Bristol-Myers Squibb (Redwood City, CA).

Statistics

P values described in the in vitro assays are based on Student *t*-tests (2-tailed; $\alpha = 0.05$) or on analysis of variance. *P* values are provided for each figure. Kaplan-Meier curve was obtained using GraphPad Prism and *P* values were calculated based on log-rank test.

Results

C1013G/CXCR4 variant occurs in patients with lymphoplasmacytic lymphoma/WM

We have investigated the presence of the C1013/CXCR4 variant in 429 patients with different B-cell lymphoproliferative disorders and found that the variant is occurring in 28.2% of WM patients (37/131) and in 20% of IgM-MGUS patients (8/40). In addition, the variant was detected in 7% of patients with splenic marginal zone lymphoma (1/14) and 1.3% of patients with diffuse large B-cell lymphoma (1/75), whereas it was absent in B-cell chronic lymphocytic leukemia, hairy cell leukemia, multiple myeloma, and IgG/IgA MGUS (Table 1), suggesting that the potential role of this variant in supporting the molecular pathogenesis of WM as well as of the IgM MGUS precursor stage. The C1013G/CXCR4 variants results in a single nucleotide change C→G, in CXCR4 leading to a predicted stop codon in place of a serine at amino acid position 338 (S338X). This has been previously linked to truncation of the C-terminal domain of the CXCR4,[19] leading to its impaired intracellular translocation. To further prove that the observed variant may indeed induce CXCR4 changes on the surface of WM cells, we evaluated the CXCR4 surface expression on independent primary WM patient BM-derived $CD19^+$ cells, either carrying the variant (n = 3) or not (n = 8), and found a higher surface expression in patients harboring the C1013G/CXCR4 variant compared with wild-type/CXCR4 patients (Figure 1A). Moreover, 10 patients with confirmed extramedullary WM histological diagnosis have also been evaluated for the presence of the somatic variant: patients with lung (3/3) and kidney (1/1) involvement presented with mutated C1013G/CXCR4, being absent in small bowel (2/2) and soft tissues (4/4), as documented by allele-specific PCR (Figure 1B), indicating that this mutation may be more prevalent in patients with extramedullary involvement.

C1013G/CXCR4 variant induces WM progression and modulates drug resistance

We aimed to dissect the in vivo functional relevance of the C1013G/CXCR4 variant in supporting WM biology. We first generated CXCR4 (GFP^+) overexpressing WM cells ($CXCR4^+$), and looked at the functional relevance of CXCR4 in WM in vivo. The efficiency of the infection was confirmed by using qRT-PCR and immunofluorescence imaging (supplemental Figure 1A,B). Both $CXCR4^+$/GFP^+ cells and empty vector/RFP^+ cells were injected into SCID/Bg mice. Because of disease progression, mice were euthanized after 3 weeks, demonstrating that the overexpression of CXCR4 in WM cells led to a more aggressive phenotype as documented by a significantly higher involvement of organs in $CXCR4^+$ cell–injected mice compared with empty vector cell–injected mice ($P < .01$; supplemental Figure 1C-E). Ex vivo studies demonstrated that $CXCR4^+$ WM cells disseminated and proliferated more rapidly in the BM and other organs including the liver and kidneys (Figure 2A-C; supplemental Figure 1C-E; $P < .01$). Moreover, these findings were also confirmed by immunofluorescence imaging, showing higher infiltration of GFP^+ compared with RFP^+ cells, which are representative of $CXCR4^+$ and empty vector infected cells, respectively (Figure 2D). Importantly, we found reduced survival in CXCR4+ cell–harboring mice compared with empty vector cell–injected ones ($P = .02$; Figure 2E). In addition, $CXCR4^+$ cell–injected mice presented with an increased serum IgM secretion, compared with either uninjected or empty vector cell–injected mice (supplemental Figure 1F). We also confirmed the presence of $CXCR4^+$ cells ex vivo by performing qRT-PCR on the BM cells harvested from the femurs of either $CXCR4^+$ cell– or empty vector–injected mice (supplemental Figure 1G). We next delineated the in vitro sequelae resulting from CXCR4 gain of function in WM cells by comparing $CXCR4^+$ cells to CXCR4 knock-down cells. Efficiency of infection was confirmed at the messenger RNA (mRNA) level and by using immunofluorescence imaging (supplemental Figure 2A-B). We found that the ability of WM cells to adhere to primary WM BM-MSCs and to proliferate when in the context of BM-MSCs was enhanced in $CXCR4^+$ WM cells and inhibited in the case of CXCR4 knock-down WM cells (Figure 2F-G). Similarly, CXCR4 overexpression led to increased adhesion capabilities of WM cells to fibronectin, as opposed to CXCR4-silenced cells that presented with inhibited WM cell adhesion to fibronectin (supplemental Figure 2C-D). Taken together, these findings indicate that CXCR4 is crucial in facilitating in vivo WM cell growth and dissemination.

We next elucidated whether the C1013G/CXCR4 variant may actively support WM pathogenesis leading to disease progression. We therefore generated stably C1013G-mutated BCWM1 cells (C1013GCXCR4-WM). Control vector–infected WM cells were used as control. The mutagenesis efficiency was confirmed at genomic DNA level and at the complementary DNA level by using quantitative PCR and qRT-PCR, respectively (supplemental Figure 3A,B).

The in vivo phenotype induced by WM cells harboring the mutation was subsequently examined. Mice injected with C1013G/CXCR4-WM cells presented with a significant dissemination of tumor cells to distant organs and increased serum IgM secretion (supplemental Figure 3C), thus recapitulating the effect observed in mice injected with $CXCR4^+$ overexpressing WM cells. In addition to the already demonstrated involvement of liver, kidney, and BM, C1013G/CXCR4-WM cell-injected mice presented with enlarged lymph nodes and lung involvement. Dissemination to central nervous system was not documented. Histopathology analysis indeed showed the presence of CXCR4- and CD20-positive cells in all tissues examined, with the exception of the brain (Figure 3A-E; supplemental Figure 3D); and the CXCR4 and CD20 positivity was higher in C1013G/CXCR4-WM cell– compared with control cell–injected mice ($P < .05$; supplemental Figure 4). Importantly, C1013G/CXCR4-WM cell-injected mice presented with decreased overall survival ($P = .003$; Figure 3F).

C1013G/CXCR4-WM cells (BCWM.1) were further characterized in vitro, showing increased adhesion and cell proliferation in the presence of primary WM BM-MSCs, thus confirming the C1013G/CXCR4 variant was able to reproduce the effects because of the overexpression of CXCR4 in WM cells (Figure 3G-H). Similar findings were validated using a different WM cell line (MWCL1; supplemental Figure 5A-B).

To better explain the ability of C1013G/CXCR4 variant to facilitate in vivo WM cell dissemination, mutated cells were characterized at the mRNA level. By performing GSEA, we demonstrated that

A

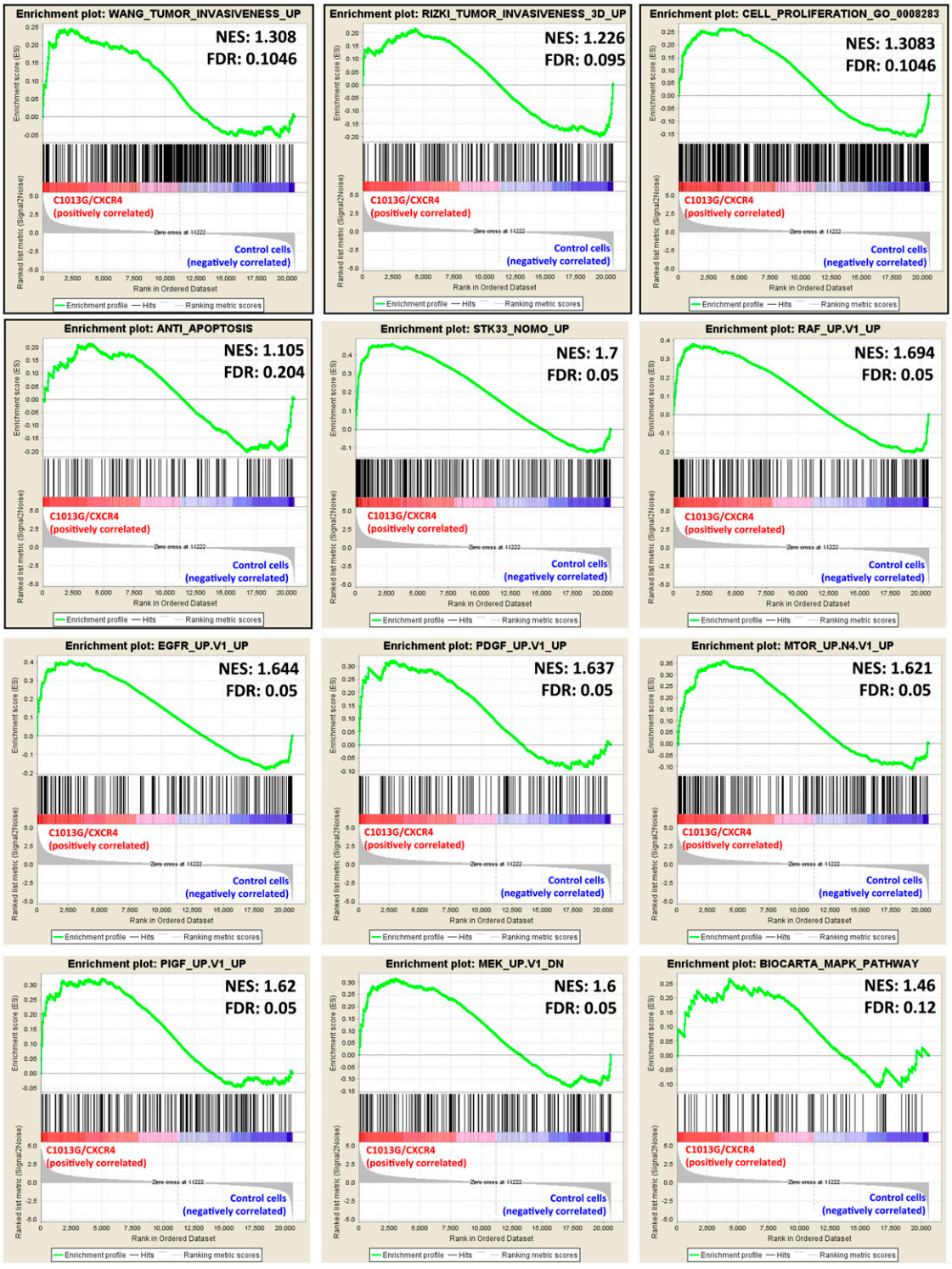

Figure 4. C1013G/CXCR4-mutated cells differ from the control cells at gene level. (A) GSEA enrichment plots of tumor invasiveness, cell proliferation, antiapoptosis, and oncogenic signature genes in C1013G/CXCR4-mutated cells vs control vector–infected cells (control cells). The green curves show the enrichment score and reflects the degree to which each gene (black vertical lines) is represented at the top or bottom of the ranked gene list. The heat map indicates the relative abundance (red to blue) of the genes specifically enriched in the mutated cells as compared with the control cells. All the gene sets were enriched in C1013G/CXCR4-mutated cells, with an FDR always <0.25. Normalized enrichments score (NES) and FDR are shown per each gene set analyzed. (B) Upregulation of genes in WM patients harboring the C1013G/CXCR4 mutation (n = 10) compared with CXCR4/wild-type WM patients (n = 30). *P* indicates *P* value. (C) GSEA enrichment plot for the upregulated genes listed in panel B, in C1013G/CXCR4-mutated cells vs control vector–infected cells (control cells). The same genes were enriched in mutated cells as compared with control cells.

B

GENE	FOLD CHANGE (WM patients C1013G/CXCR4 vs unmutated)	*P*-VALUE
ARID1A	2,388	0.02
BLNK	5,598	0.012
BTK	2,291	0.019
CCND1	5,567	0.026
CD79A	2,021	0.049
CTNNBL1	1,989	0.046
GSK3B	2,288	0.014
IRAK4	2,413	0.029
IRF3	3,595	0.027
ITPR1	2,824	0.018
MAP3K1	1,809	0.010
MAP3K7	3,004	0.002
MAPK14	1,566	0.039
MAPK1	2,039	0.012
MAPK8	1,628	0.032
NREP	2,359	0.038
OSBPL3	3,178	0.025
PAX5	1,911	0.016
PI3KCB	2,228	0.023
POU2AF1	2,198	0.046
RAF1	1,618	0.023
RELA	1,809	0.036
SMEK1	2,152	0.014

C

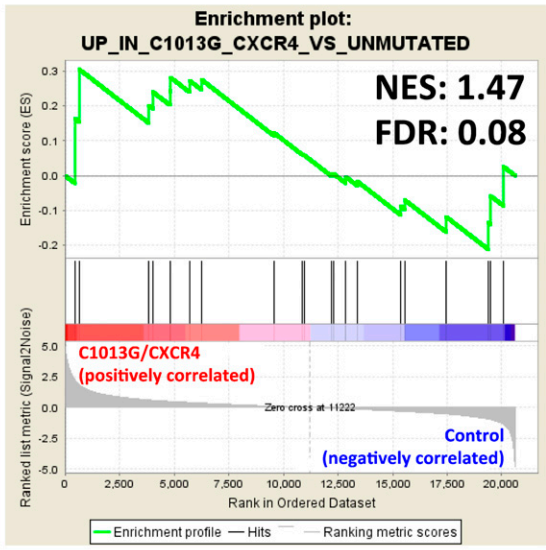

Figure 4. (Continued).

genes related to invasiveness, cell proliferation, antiapoptosis, and genes known to be oncogenic were all enriched in C1013G/CXCR4-WM cells compared with the WM control vector–infected cells,[20,21] thus explaining the more aggressive phenotype of mutated cells compared with the control cells (Figure 4A). These in vivo observations together with the changes observed at mRNA level indicate that C1013G/CXCR4-WM variant acts as an activating mutation in WM cells. We profiled WM patients at mRNA levels using qRT-PCR and found that several genes related to the mitogen-activated protein kinase, BTK, and PI3K pathways, that are known to support WM biology,[22,23] were significantly upregulated in C1013G/CXCR4-mutated WM patients (n = 10) compared with CXCR4/wild-type WM patients (n = 30) (Figure 4B). Importantly, those changes were equally enriched in C1013G/CXCR4-mutated BCWM1 cells compared with the control vector–infected cells, thus further confirming that the C1013G/CXCR4 engineered BCWM1 cells are representative for what observed in primary WM tumor cells (Figure 4C).

We next interrogated whether WM cells harboring the C1013G/CXCR4 variant might present with altered sensitivity to conventionally used anti-WM small molecules. GSEA studies showed that genes related to drug resistance were enriched in WM cell line harboring the mutation, whereas genes related to drug responsiveness were enriched in WM control cells (Figure 5A). This prompted us to investigate whether novel anti-WM agents may alter their antitumor efficacy in the context of CXCR4-mutated WM cells; we found that WM cells harboring the C1013G/CXCR4 somatic variant presented with resistance to BTK as well as PI3K and mTOR inhibitors (Figure 5B-D). These data are in support of recent data indicating that WM patients with WHIM-like mutated CXCR4 presented with resistance to Ibritunib-based therapy.[24] Importantly, proteasome inhibitors were equally effective in exerting toxicity against both C1013G/CXCR4-mutated WM cells and control cells (Figure 5E-F).

Anti-CXCR4 monoclonal antibody, BMS-936564/MDX-1338 exerts antitumor activity against wild-type and C1013G/CXCR4-mutated WM cells

Based on the biological relevance of CXCR4 in supporting WM progression, we tested an anti-CXCR4 monoclonal antibody for its activity in targeting WM cells. We have found that BMS-936564/MDX-1338 was able to inhibit migration of WM cell lines toward either primary WM BM-MSCs or SDF-1 (supplemental Figure 6A-B). Similarly, BMS-936564/MDX-1338–dependent inhibition of

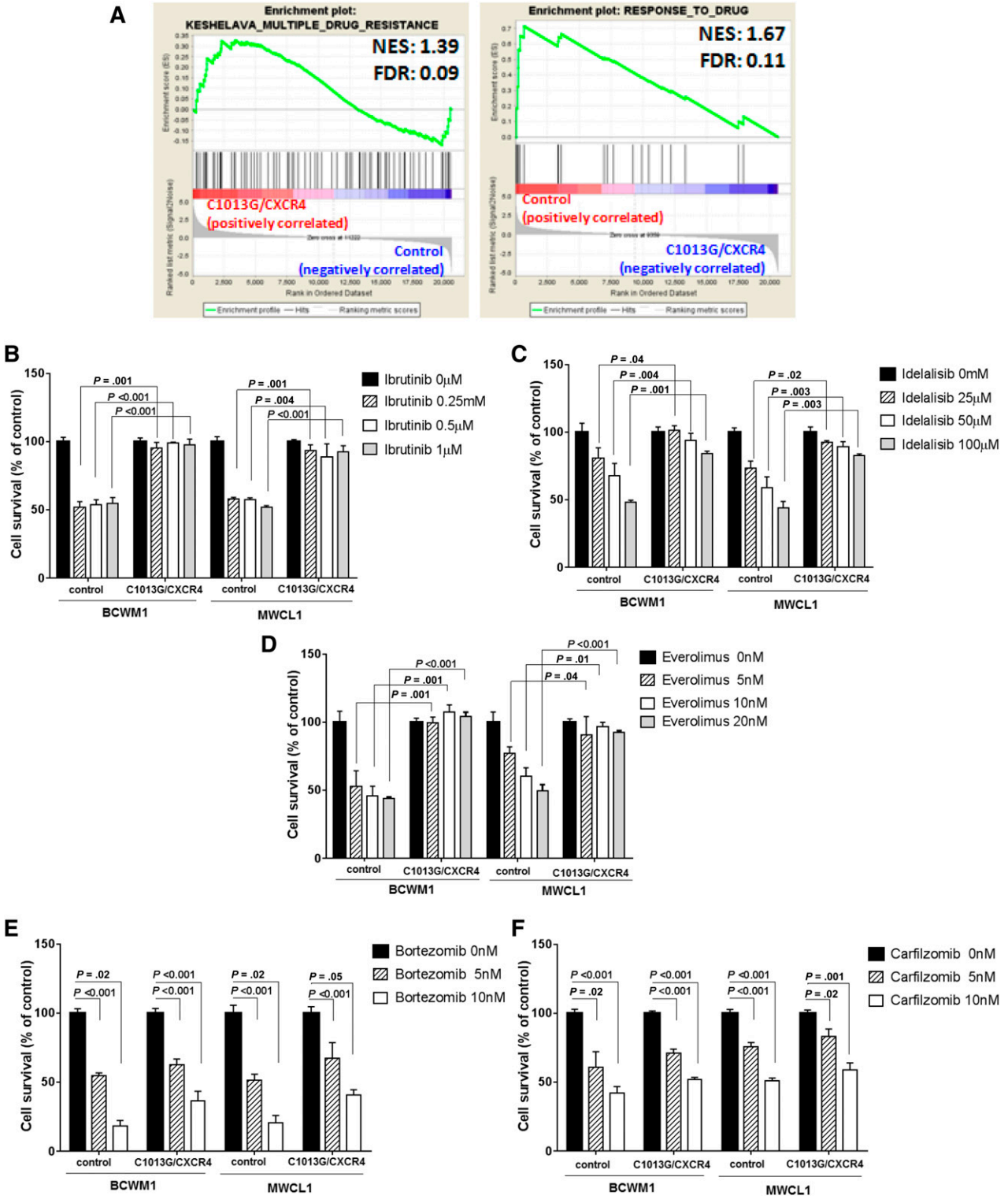

Figure 5. WM cells harboring the C1013G/CXCR4 somatic variant present with drug resistance. (A) GSEA enrichment plots of multiple drug resistance and response to drug signature genes in C1013G/CXCR4-mutated cells and control vector–infected cells (control cells), respectively. The green curves show the enrichment score and reflects the degree to which each gene (black vertical lines) is represented at the top or bottom of the ranked gene list. The heat map indicates the relative abundance (red to blue) of the genes specifically enriched in the mutated cells as compared with the control cells. Gene sets were considered enriched with an FDR always <0.25. Normalized enrichments score (NES) and FDR are shown per each gene set analyzed. (B-F) C1013G/CXCR4 WM cell lines (BCWM1; MWCL1) or control vector–infected cells (control) were exposed to everolimus, ibrutinib, idelalisib, bortezomib, and carfilzomib for 48 hours. Cytotoxicity was determined by 3-(4,5-dimethylthiazol-2-yl)-2,5-diphenyltetrazolium bromide.

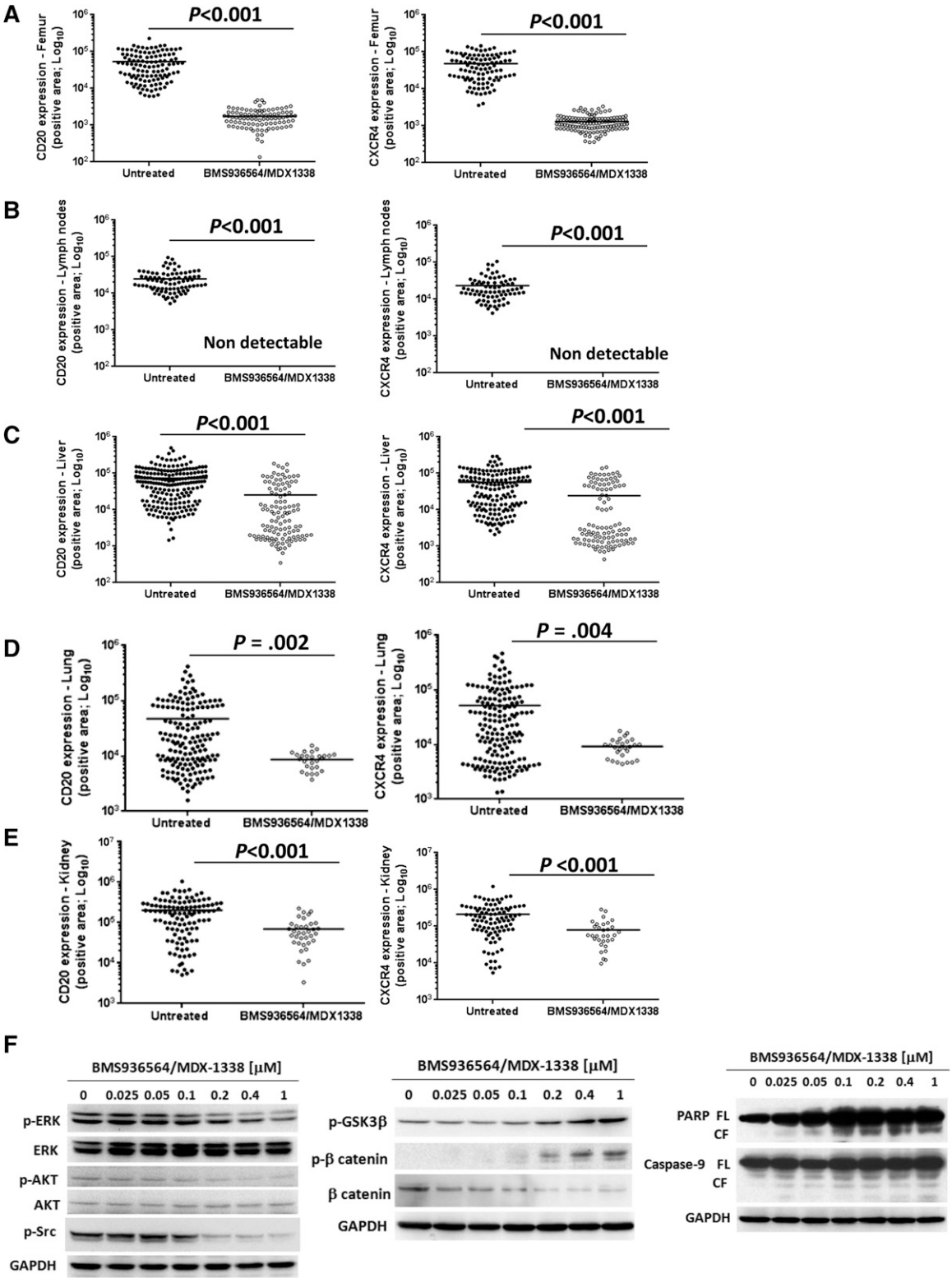

Figure 6. BMS936564-MDX1338 targets C1013G/CXCR4-mutated cells in vivo and targets survival- and apoptosis-related signals in WM cells. (A-E) BMS936564-MDX1338 inhibited dissemination of C1013G/CXCR4-mutated WM cells in vivo. Human CD20 and CXCR4 staining was significantly reduced in tissues explanted from mice treated with BMS936564/MDX1338 compared with isotype control-treated mice (untreated). *P* indicates *P* values. Representative immunohistochemistry images are shown in supplemental Figure 6. (F) C1013G/CXCR4-mutated cells have been cultured in presence or absence of BMS936564/MDX-1338 for 6 hours, showing inhibition of phospho (p)-ERK, ERK, *p*-AKT, AKT, and *p*-Src. Similarly, cells were exposed to the compound for 14 hours, and induction of apoptosis-related pathways was documented (*p*-GSK3β, *p*-β catenin, PARP, and Caspase-9).

WM cell adhesion to WM BM-MSCs and inhibition of WM cells proliferation in presence of WM BM-MSCs was demonstrated (supplemental Figure 6C-E). To dissect the possible role of BMS-936564/MDX-1338 in affecting WM signaling, we cultured WM cells in absence or presence of primary WM BM-MSCs, with increasing concentration of the anti-CXCR4 antibody, and found a drug-dependent inhibition of *p*-Akt and *p*-Src in WM cells cultured in the context of BM-MSCs, thus suggesting the ability of BMS-936564/MDX-1338 to target WM cells even in the context of BM milieu (supplemental Figure 6F). Isotype control did not exert any effect on adhesion and migration of WM cells in vitro (supplemental Figure 6G,H). BMS-936564/MDX-1338 may exert a pro-apoptotic effect in B-cell malignancies[25]; therefore, we exposed WM cells to BMS-936564/MDX-1338 and found an increase of caspase-9 and PARP cleavage (supplemental Figure 6I).

The interaction between SDF1/CXCR4 and β-catenin has been previously shown in models of metastatic solid tumors.[26] In addition, phosphorylated-GSK3β is known to facilitate β-catenin degradation.[26,27] We therefore investigated the effect of BMS-936564/MDX-1338 on β-catenin and found that by neutralizing CXCR4 with BMS-936564/MDX-1338, WM cells present with increased phospho(p)-GSK3-β, and *p*-β-catenin upregulation, leading to β-catenin degradation (supplemental Figure 6I). These findings may explain, at least in part, the possible mechanisms of BMS-936564/MDX-1338-induced apoptosis in WM cells.

We next examined the role of BMS-936564/MDX-1338 in CXCR4-mutated WM cells in vivo. BMS-936564/MDX-1338 inhibited WM dissemination in mice injected with C1013G/CXCR4 WM cells as shown by significant reduction of $CXCR4^+/CD20^+$ cell infiltration in femur, liver, kidney, and lung in treated mice compared with control Ab-treated mice (Figure 6A-E; supplemental Figure 7A-D). Importantly, involvement of lymph nodes was absent in mice treated with BMS-936564/MDX-1338 (supplemental Figure 7E). These findings were further confirmed in vitro. We found that BMS-936564/MDX-1338 was equally active in targeting adhesion, migration, and proliferative properties of CXCR4-mutated cells in the context of the BM microenvironment (supplemental Figure 8A-D). Importantly, BMS-936564/MDX-1338 increased caspase-9 and PARP cleavage in CXCR4-mutated WM cells; and it also modulated the GSK3-β/β-catenin signaling, leading to upregulation of *p*-GSK3-β/*p*-β-catenin and β-catenin degradation. In addition, BMS-936564/MDX-1338 induced a dose-depend inhibition of *p*-extracellular signal-regulated kinase (*p*-ERK), *p*-Akt, and *p*-Src in WM cells harboring the *C1013G/CXCR4* variant (Figure 6F).

The anti-WM activity of BMS-936564/MDX-1338 was also tested in vivo, using wild-type WM cells. $BCWM.1\text{-}mCherry^+$ cells were injected IV into SCID/Bg mice and treated mice with either BMS-936564/MDX-1338 or control antibody. BM, spleen, and lymph nodes were harvested demonstrating the ability of BMS-936564/MDX-1338 to inhibit WM cell dissemination as documented ex vivo by using immunofluorescence imaging (supplemental Figure 9A).

Discussion

We examined 429 patients with B-cell lymphoproliferative disorders and found that 28% of patients with low-grade lymphoplasmacytic lymphoma (WM) present with the C1013G/CXCR4 variant. We next aimed to dissect the functional relevance of C1013G/CXCR4 variant, to evaluate its putative role in mediating WM cell dissemination and disease progression using in vivo models, and to identify novel therapeutic approaches that may target the C1013G/CXCR4-mutated lymphoplasmacytic cells. These studies demonstrated that CXCR4 plays a crucial role supporting WM cell homing to the BM as well as WM dissemination to distant organs, as shown in vivo by using CXCR4 gain-of-function studies. Importantly, WM cells harboring the C1013G/CXCR4 variant exerted a similar phenotype compared with the CXCR4-overexpressing cells, thus suggesting that the C1013G/CXCR4 variant may represent a functionally active mutation. Moreover, the C1013G/CXCR4-mutated cells showed dissemination to lymph nodes, in vivo, compared with either the control cells or the CXCR4-overexpressing WM cells, thus suggesting that the generated C1013G/CXCR4 variant was able to recapitulate what was observed clinically in patients. Importantly, C1013G/CXCR4-mutated cells were able to colonize extramedullary tissues, such as lung and kidney in vivo, reflecting the observed phenotype in patients with extramedullary WM, where the variant has been detected in all the cases of lung and kidney involvement.

The observed C1013G/CXCR4 variant is 1 of the mutations originally described in WHIM syndrome. This is a rare, inherited, heterozygous, autosomal dominant disease characterized by aberrantly functioning immunity. It is caused by mutations of CXCR4, responsible for the truncation of the carboxyterminal talk (C-tail) of the receptor that impairs its intracellular trafficking, leading to increased responsiveness to chemokine ligand and retention of neutrophils in BM.[7,8,28,29] Recent evidence has documented the presence of this variant in WM patients[9]; nevertheless, the in vivo functional sequelae of this mutation in WM, and whether the somatic variant occurs in other B-cell lymphoproliferative disorders where CXCR4 mediates tumor cell trafficking and dissemination, has not been previously described. The increased ability of C1013G/CXCR4-mutated cells to disseminate in vivo leading to disease progression was supported by enrichment of genes related to cell invasiveness, anti-apoptosis, cell proliferation, and oncogenesis. This resulted in the upregulation of pro-survival pathways in mutated cells compared with control cells. These effects were reverted when WM-harboring mice, injected with either C1013G/CXCR4-mutated cells or control cells, had been treated with the monoclonal antibody anti-CXCR4. BMS-936564/MDX-1338 was able to target WM cells, independently of their mutational status, with inhibited activation of pro-survival signaling pathways, proapoptotic cascades, together with inhibited WM cells dissemination in vivo. Of note, the C1013G/CXCR4 somatic variant was also associated with WM cell resistance to mTOR, PI3K, and BTK inhibitors, thus supporting the role of this variant in mediating drug resistance. In contrast, C1013G/CXCR4-mutated WM cells were equally sensitive to both bortezomib and carfilzomib, thus suggesting the possible combinatory regimen of BMS936564/MDX-1338 with proteasome inhibitors in WM patients harboring the C1013G/CXCR4 somatic variant. We hypothesize that BTK, PI3K, and mTOR inhibitors were not effective against mutated cells because of the upregulation of genes related to those specific pathways. Moreover, we could confirm that mutated CXCR4 cells presented with enrichment of RAF as well as mitogen-activated protein kinase/mitogen-activated protein kinase kinase and mTOR pathways, thus further suggesting the presence of crosstalk between RAF and mitogen-activated protein kinase kinase/ERK/mTOR pathways.[30-32] In contrast, NF-κB and NF-κB–related apoptotic genes were not differentially modulated in CXCR4-mutated cells compared with control cells (data not shown). This may explain, at least in part, the presence of BTK-, mTOR-, and PI3K-inhibitor resistance and sensitivity to proteasome inhibitors in mutated WM cells compared with wild-type cells. Further studies are

required to better define the role of C1013G/CXCR4-mediated drug resistance.

Our findings indicate that clonal WM cells harbor mutation in the CXCR4 gene, which is functionally active in this disease, as demonstrated in vivo. Moreover, we may specifically target CXCR4, either wild-type or C1013G/CXCR4 mutated, resulting in inhibition of WM cell dissemination in vivo, providing the basis for translating these observations into clinical trials for WM patients used either alone or in proteasome inhibitor-based regimen.

Acknowledgments

This work was supported in part by research grants from the International Waldenström's Macroglobulinemia Foundation, the Leukemia & Lymphoma Society, The Kirsch Laboratory for Waldenström, and the Heje Fellowship.

Authorship

Contribution: A.M.R. and A.S. designed the experiments, performed in vivo studies, and wrote the manuscript; P.M. performed gene expression studies; M.M., Y.M., and Y.A. supervised in vivo studies and immunohistochemistry studies; M.K., P.C., and L.C. provided BMS-936564/MDX1338 and the related isotype control antibody; I.S. performed drug sensitivity assays; J.F.S.M., R.G.-S., and C.J. provided patient samples, performed allele-specific polymerase chain reaction for detecting the C1013G/CXCR4 variant, and revised the manuscript; and I.M.G. supervised all aspects of the project and edited the manuscript.

Conflict-of-interest disclosure: M.K., P.C., and L.C. are employees at Bristol-Myers Squibb. The remaining authors declare no competing financial interests.

Correspondence: Irene M. Ghobrial, Medical Oncology, Dana-Farber Cancer Institute, 450 Brookline Ave, Boston, MA, 02115; e-mail: irene_ghobrial@dfci.harvard.edu.

References

1. Treon SP, Xu L, Yang G, et al. MYD88 L265P somatic mutation in Waldenström's macroglobulinemia. *N Engl J Med.* 2012;367(9): 826-833.
2. Yang G, Zhou Y, Liu X, et al. A mutation in MYD88 (L265P) supports the survival of lymphoplasmacytic cells by activation of Bruton tyrosine kinase in Waldenström macroglobulinemia. *Blood.* 2013;122(7): 1222-1232.
3. Leleu X, Eeckhoute J, Jia X, et al. Targeting NF-kappaB in Waldenström macroglobulinemia. *Blood.* 2008;111(10):5068-5077.
4. Roccaro AM, Sacco A, Chen C, et al. microRNA expression in the biology, prognosis, and therapy of Waldenström macroglobulinemia. *Blood.* 2009; 113(18):4391-4402.
5. Ghobrial IM, Gertz MA, Fonseca R. Waldenström macroglobulinaemia. *Lancet Oncol.* 2003;4(11): 679-685.
6. Vijay A, Gertz MA. Waldenström macroglobulinemia. *Blood.* 2007;109(12): 5096-5103.
7. Balabanian K, Lagane B, Pablos JL, et al. WHIM syndromes with different genetic anomalies are accounted for by impaired CXCR4 desensitization to CXCL12. *Blood.* 2005;105(6):2449-2457.
8. Balabanian K, Levoye A, Klemm L, et al. Leukocyte analysis from WHIM syndrome patients reveals a pivotal role for GRK3 in CXCR4 signaling. *J Clin Invest.* 2008;118(3):1074-1084.
9. Hunter Z, Xu L, Yang G, et al. The genomic landscape of Waldenström macroglobulinemia is characterized by highly recurring MYD88 and WHIM-like CXCR4 mutations, and small somatic deletions associated with B-cell lymphomagenesis. *Blood.* 2014;123(11): 1637-1646.
10. Treon SP, Cao Y, Xu L, Yang G, Liu X, Hunter ZR. Somatic mutations in MYD88 and CXCR4 are determinants of clinical presentation and overall survival in Waldenström's macroglobulinemia [published online ahead of print February 19, 2014]. *Blood.* doi:10.1182/blood-2014-01-550905.
11. Campo E, Swerdlow SH, Harris NL, Pileri S, Stein H, Jaffe ES. The 2008 WHO classification of lymphoid neoplasms and beyond: evolving concepts and practical applications. *Blood.* 2011; 117(19):5019-5032.
12. Paiva B, Montes MC, Garcia-Sanz R, et al. Multiparameter flow cytometry for the identification of the Waldenström's clone in IgM-MGUS and Waldenström's macroglobulinemia: new criteria for differential diagnosis and risk stratification. *Leukemia.* 2014;28(1):166-173.
13. van Dongen JJ, Lhermitte L, Böttcher S, et al; EuroFlow Consortium (EU-FP6, LSHB-CT-2006-018708). EuroFlow antibody panels for standardized n-dimensional flow cytometric immunophenotyping of normal, reactive and malignant leukocytes. *Leukemia.* 2012;26(9): 1908-1975.
14. Roccaro AM, Sacco A, Maiso P, et al. BM mesenchymal stromal cell-derived exosomes facilitate multiple myeloma progression. *J Clin Invest.* 2013;123(4):1542-1555.
15. Subramanian A, Tamayo P, Mootha VK, et al. Gene set enrichment analysis: a knowledge-based approach for interpreting genome-wide expression profiles. *Proc Natl Acad Sci USA.* 2005;102(43):15545-15550.
16. Roccaro AM, Sacco A, Husu EN, et al. Dual targeting of the PI3K/Akt/mTOR pathway as an antitumor strategy in Waldenström macroglobulinemia. *Blood.* 2010;115(3):559-569.
17. Sacco A, Aujay M, Morgan B, et al. Carfilzomib-dependent selective inhibition of the chymotrypsin-like activity of the proteasome leads to antitumor activity in Waldenström's Macroglobulinemia. *Clin Cancer Res.* 2011;17(7): 1753-1764.
18. Azab F, Azab AK, Maiso P, et al. Eph-B2/ephrin-B2 interaction plays a major role in the adhesion and proliferation of Waldenström's macroglobulinemia. *Clin Cancer Res.* 2012;18(1): 91-104.
19. Alapi K, Erdos M, Kovács G, Maródi L. Recurrent CXCR4 sequence variation in a girl with WHIM syndrome. *Eur J Haematol.* 2007;78(1):86-88.
20. Rizki A, Weaver VM, Lee SY, et al. A human breast cell model of preinvasive to invasive transition. *Cancer Res.* 2008;68(5):1378-1387.
21. Wang W, Wyckoff JB, Goswami S, et al. Coordinated regulation of pathways for enhanced cell motility and chemotaxis is conserved in rat and mouse mammary tumors. *Cancer Res.* 2007; 67(8):3505-3511.
22. Chng WJ, Schop RF, Price-Troska T, et al. Gene-expression profiling of Waldenström macroglobulinemia reveals a phenotype more similar to chronic lymphocytic leukemia than multiple myeloma. *Blood.* 2006;108(8): 2755-2763.
23. Gutiérrez NC, Ocio EM, de Las Rivas J, et al. Gene expression profiling of B lymphocytes and plasma cells from Waldenström's macroglobulinemia: comparison with expression patterns of the same cell counterparts from chronic lymphocytic leukemia, multiple myeloma and normal individuals. *Leukemia.* 2007;21(3): 541-549.
24. Treon SP, Tripsas CK, Yang G, et al. A prospective multicenter study of the bruton's tyrosine kinase inhibitor ibrutinib in patients with relapsed or refractory Waldenström's macroglobulinemia [abstract]. *Blood;* 2013; 122(21). Abstract 251.
25. Kuhne MR, Mulvey T, Belanger B, et al. BMS-936564/MDX-1338: a fully human anti-CXCR4 antibody induces apoptosis in vitro and shows antitumor activity in vivo in hematologic malignancies. *Clin Cancer Res.* 2013;19(2): 357-366.
26. Wang L, Li CL, Wang L, et al. Influence of CXCR4/SDF-1 axis on E-cadherin/β-catenin complex expression in HT29 colon cancer cells. *World J Gastroenterol.* 2011;17(5):625-632.
27. Polakis P. More than one way to skin a catenin. *Cell.* 2001;105(5):563-566.
28. Hernandez PA, Gorlin RJ, Lukens JN, et al. Mutations in the chemokine receptor gene CXCR4 are associated with WHIM syndrome, a combined immunodeficiency disease. *Nat Genet.* 2003;34(1):70-74.
29. Taniuchi S, Masuda M, Fujii Y, Izawa K, Kanegane H, Kobayashi Y. The role of a mutation of the CXCR4 gene in WHIM syndrome. *Haematologica.* 2005;90(9):1271-1272.
30. Downward J. Targeting RAS signalling pathways in cancer therapy. *Nat Rev Cancer.* 2003;3(1): 11-22.
31. Downward J. Targeting RAS and PI3K in lung cancer. *Nat Med.* 2008;14(12):1315-1316.
32. Lim KH, Counter CM. Reduction in the requirement of oncogenic Ras signaling to activation of PI3K/AKT pathway during tumor maintenance. *Cancer Cell.* 2005;8(5):381-392.

2014 123: 4120-4131
doi:10.1182/blood-2014-03-564583 originally published online April 7, 2014

C1013G/CXCR4 acts as a driver mutation of tumor progression and modulator of drug resistance in lymphoplasmacytic lymphoma

Aldo M. Roccaro, Antonio Sacco, Cristina Jimenez, Patricia Maiso, Michele Moschetta, Yuji Mishima, Yosra Aljawai, Ilyas Sahin, Michelle Kuhne, Pina Cardarelli, Lewis Cohen, Jesus F. San Miguel, Ramon Garcia-Sanz and Irene M. Ghobrial

Blood (print ISSN 0006-4971, online ISSN 1528-0020), is published weekly by the American Society of Hematology, 2021 L St, NW, Suite 900, Washington DC 20036.